

Imprint of a Steep Equation of State in the growth of structure

Mariana Jaber-Bravo,* Erick Almaraz,† and Axel de la Macorra
*Instituto de Física, Universidad Nacional Autónoma de México,
 A.P. 20-364 CDMX 01000, México.*

(Dated: June 25, 2019)

We study the cosmological properties of a dynamical of dark energy (DE) component determined by a Steep Equation of State (SEoS) $w(z) = w_0 + w_i \frac{(z/z_T)^q}{1+(z/z_T)^q}$. The SEoS has a transition at z_T between two pivotal values (w_i, w_0) which can be taken as an early time and present day values of w and the steepness is given by q . We describe the impact of this dynamical DE at background and perturbative level. The steepness of the transition has a better cosmological fit than a conventional CPL model with $w = w_0 + w_a(1 - a)$. Furthermore, we analyze the impact of steepness of the transition in the growth of matter perturbations and structure formation. This is manifest in the linear matter power spectrum, $P(k)$, the logarithmic growth function, $f\sigma_8(z)$, and the differential mass function $dn/d\log M(z=0)$. The differences in these last three quantities is at a percent-level using the same cosmological baseline parameters in our SEoS and a Λ CDM model. However, we find an increase in the power spectrum, producing a bump at $k \approx k_T$ with $k_T \equiv a_T H(a_T)$ the mode associated to the time of the steep transition ($a_T = 1/(1+z_T)$). Different dynamics of DE lead to a different amount of DM at present time which has an impact in Power Spectrum and accordingly in structure formation.

I. INTRODUCTION

The standard Λ CDM paradigm is based on the assumptions of homogeneity and isotropy of the Universe at large scales, the validity of General Relativity and the cosmological constant term as cause of the accelerated cosmic expansion. Although it has been proven successful when tested against observations it faces some major theoretical issues such as the extreme fine-tuning problem known as the cosmological constant problem [1] which leads to the necessity of extending it. Some candidates include scalar field models or modifications of General Relativity

Observational probes coming from different physical phenomena such as the temperature and polarization of cosmic microwave background (CMB) [2], the luminosity distance of supernovae [3] or the statistical signature of the baryonic acoustic oscillations (BAO) from galaxy surveys [4–8], quasars [9, 10] or voids [11], have improved significantly over the years.

In this work we choose to focus on an effective model of a fluid with free parameters. In this, we consider the dark energy (DE) contribution, ρ_{DE} to be a perfect fluid so dissipative terms will not be present. In this situation we describe the dynamics of this component through its equation of state, $w(z)$, defined by:

$$p_{DE}(\rho_{DE}) = w(z)\rho_{DE}(z) \quad (1)$$

which can be parameterized to match observations.

Several proposals for $w(z)$ can be found in the literature [12–26]. These proposals attempt to describe the dynamics of dark energy without assuming a particular theoretical model, but providing practical parametrizations that can be readily confronted against observations. In this approach, a cosmological constant solution can be modelled as a fluid with pressure $p_\Lambda = -\rho_\Lambda$, which implies an equation of state $w = -1$. This landscape has recently been extended to cover the background expansion rate as prescribed by $f(R)$ theories [27].

The study of the perturbative regime could potentially be used to discriminate between a cosmological constant and models with a negative pressure component from Modified gravity. In this pursue, ongoing and upcoming surveys such as eBOSS [28], DESI [29], LSST [30] and EUCLID [31] will provide extremely precise measurements of the growth of structure in the Universe, which in turn, will allow to probe the nature of the cosmic acceleration mechanism.

Studying the effect of dynamical DE into the clustering at large scales is thus a relevant task for the cosmological community. In this work we present the implications that a steep transition in the DE EoS, $w(z)$ has in the growth of structure.

This paper is organized as follows. In Section II we describe our model for dark energy, the cosmology chosen and the analytical treatment used for the perturbations. Section III comprises our main results in the particular case of a smooth dark energy component and its impact on linear observables in the perturbative regime. Our conclusions and outlook are covered in section IV.

* jaber@fisica.unam.mx

† ealmaraz@estudiantes.fisica.unam.mx

II. METHODS

A. Steep Equation of State

In a previous work [32] we presented a parametric form for $w(z)$ inspired in quintessence fields and tested its free parameters with observations such as the Baryon Acoustic Oscillations (BAO) peak measured in galaxies or in the Lyman- α forest, as well as the compressed Cosmic Microwave Background likelihood [33, 34], and the local determination of H_0 included in [35].

Our form for the equation of state is:

$$w(z) = w_0 + (w_i - w_0) \frac{(z/z_T)^q}{1 + (z/z_T)^q} \quad (2)$$

which allows for a steep transition to take place at a pivotal redshift $z = z_T$ with a steepness modulated by the exponent q . For this reason we dubbed this equation ‘‘SEoS’’ (from ‘‘Steep Equation of State’’) in this work.

We notice that in the case where the transition is smooth and occurs at a particular redshift: $z_T = q = 1$, we recover a form for the equation of state known as the Chevallier-Polarski-Linder parametrization (CPL) [12, 13] which has been widely used in the literature,

$$\begin{aligned} w(z; z_T = 1, q = 1) &= w_0 + (w_i - w_0) \frac{z}{1+z} \\ &= w_0 + w_a(1-a), \end{aligned} \quad (3)$$

where $w_a \equiv w_i - w_0$ and we keep the convention $a_0 = 1$.

In this work we will refer to the particular case of having arbitrary w_0 and w_i but taking $z_T = q = 1$, as the ‘‘CPL limit’’ of the SEoS (2).

We notice that the parameter q modulates the steepness of the transition: the greater the value for q , the more abrupt is the transition, as figure 1 shows.

B. Background models

Once we have specified the equation for the dynamics of DE, the expansion rate (for a flat Universe) is given by:

$$\frac{H(z)}{H_0} = \sqrt{\Omega_r^{(0)}(1+z)^4 + \Omega_m^{(0)}(1+z)^3 + \Omega_{DE}^{(0)}F(z)} \quad (4)$$

where $H \equiv (\frac{da}{dt})(\frac{1}{a})$ is the Hubble parameter, t the cosmic time, $a = (1+z)^{-1}$ the scale factor of the Universe and $H_0 = 100 \cdot h \text{ km} \cdot \text{s}^{-1} \text{ Mpc}^{-1}$ the Hubble

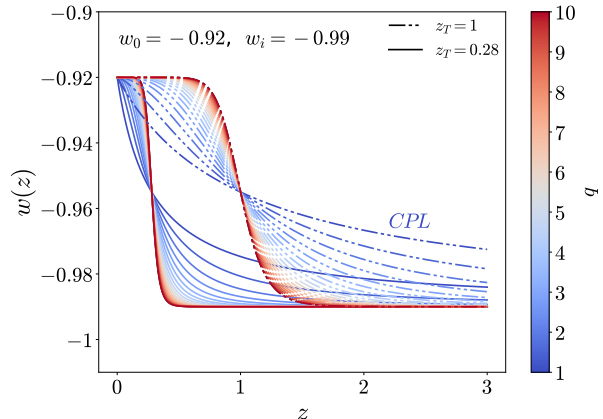


FIG. 1: [Color online] Evolution of equation (2) (‘‘SEoS’’) for different values of the transition redshift, z_T , and the steepness parameter, q . The parameters w_0 and w_i were fixed to -0.92 and -0.99 , respectively, and q was varied from $q = 1$ (blue) to $q = 10$ (red). Solid lines represent the evolution of $w(z)$ with $z_T = 0.28$, and dot-dashed lines indicate $z_T = 1$. The CPL case is explicitly labeled and corresponds to $z_T = q = 1$.

constant at present time. The fractional densities of matter, radiation and dark energy at $z = 0$, are given by $\Omega_m^{(0)}$, $\Omega_r^{(0)}$, $\Omega_{DE}^{(0)}$, respectively, which follow the flatness constraint $\Omega_m + \Omega_r + \Omega_{DE} = 1$.

The function $F(z)$ in equation (4) encodes the evolution of the DE component in terms of its equation of state:

$$\begin{aligned} F(z) &\equiv \frac{\rho_{DE}(z)}{\rho_{DE}(0)} \\ F(z) &= \exp\left(-3 \int_0^z dz' \frac{1+w(z')}{1+z'}\right) \end{aligned} \quad (5)$$

For the free parameters in equation (2) we have chosen the best fit values obtained in [32] from the combination of BAO measurements [4–7, 9, 10] and the local determination of H_0 [35]. This corresponds to: $w_0 = -0.92$, $w_i = -0.99$, $q = 9.97$ and $z_T = 0.28$. The cosmological parameters, Ω_m and H_0 , were set equal to those reported by the Planck collaboration [36], so we can compare the discrepancy arising only from the different dynamics of DE (table I, models I-III). This is $\Omega_m = 0.3089$ and $H_0 = 67.74$ ($\omega_c = 0.1198$).

However, to take into account the full result obtained in [32], we also set the values for Ω_m and H_0 to those obtained with the constraining procedure reported previously. This corresponds to the model IV from table I and values $\Omega_m = 0.3340$ and $H_0 = 73.22$ ($\omega_c = 0.1568$). This value for H_0 corresponds to the one reported in [35], which is known

Alias	w_0	w_i	q	z_T	$H_0[km/sMpc^{-1}]$	$\omega_c \equiv \Omega_c h^2$	$\Omega_m^{(0)}$
(I) Λ CDM-P	-1	-1	1	1	67.27	0.1198	0.3156
(II) $SEoS$ -P	-0.92	-0.99	9.97	0.28	67.27	0.1198	0.3156
(III) CPL -P	-0.92	-0.99	1	1	67.27	0.1198	0.3156
(IV) $SEoS$ -bf	-0.92	-0.99	9.97	0.28	73.22	0.1568	0.3340

TABLE I: Models used in this work. The cosmological parameters in models I-III correspond to Planck TT,TE,EE+lowP [36], whereas model IV has the best fit values obtained in [32]. The rest of the parameters were kept fixed for all cases: $\Omega_b h^2 = 0.02225$, $\ln(10^{10} A_s) = 3.094$, $n_s = 0.9645$, also corresponding to those reported by Planck.

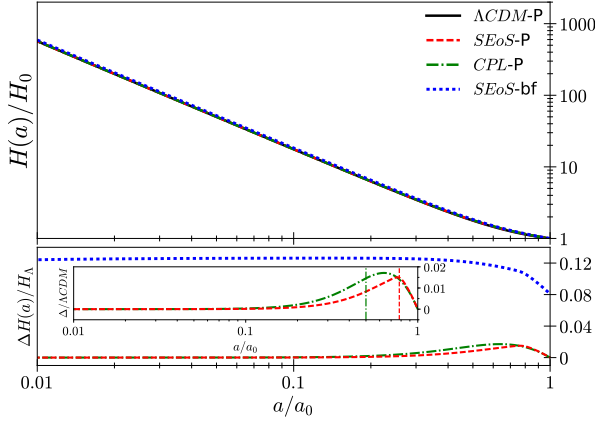


FIG. 2: [Color online] (Upper panel) Hubble expansion rate normalized to H_0 for the models described in Table I. (Bottom panel) Ratio of solutions for equation (2) to a cosmological constant: $\Delta H/H_\Lambda \equiv (H - H_\Lambda)/H_\Lambda$, where H_Λ refers to the solution Λ CDM-P. The inset plot shows only the solutions $SEoS$ -P and CPL -P compared to Λ CDM-P. The vertical lines represent the transition redshift for each model.

to be in tension with the value extrapolated from Planck measurements of CMB. This will have an impact in our analysis.

The rest of the cosmological parameters was fixed to the values from Planck TT,TE,EE+lowP [36] used in our previous analysis. In particular, we set the same primordial spectrum to focus on the effect of a late time dynamical dark energy component. This is, we set: $\ln(10^{10} A_s) = 3.094$, $n_s = 0.9645$, and $\Omega_b h^2 = 0.02225$.

C. Perturbative regime

We examine the growth of perturbations during the matter-DE domination era using “SEoS” (equation (2)) as the model for DE.

For a late time Universe we have a mixture of matter and DE and we know radiation to be subdominant. In that case the growth of over-densities can be studied in the Newtonian limit of the formalism this is, considering non-relativistic components that are well inside the horizon. For coupled fluids we have:

$$a^2 \frac{d^2 \delta_i(a)}{da^2} + a \left(3 + \frac{\dot{H}}{H^2} \right) \frac{d\delta_i(a)}{da} - \left[\frac{3}{2} \Sigma_j (\Omega_j \delta_j) - \frac{(c_s^2)_i k^2}{a^2 H^2} \delta_i(a) \right] = 0, \quad (6)$$

$i, j = \text{matter, dark energy.}$

where we have used $H^2 = \frac{8\pi G}{3} \bar{\rho}$. The density contrast of the i -th fluid is represented by $\delta_i \equiv (\rho_i - \bar{\rho})/\bar{\rho}$, where $\bar{\rho}$ is the background density, and $(c_s^2)_i$ represents the corresponding speed of sound, defined by $(c_s^2)_i \equiv \frac{\delta P_i}{\delta \rho_i}$.

We find the solutions for equation (6) in the particular case of $\delta_{DE} = 0$, this is, when DE does not cluster, since the spatial fluctuations of typical dark energy models are very much suppressed with re-

spect to those of dark matter.

In addition to finding the numerical solutions of equation (6), we also used a modified version of the Boltzmann solver CAMB [37] in which we introduced “SEoS” as the background model.

III. RESULTS

Regarding the solution for $w_{DE}(a)$ we choose to explore the different scenarios which are referenced in Table I and were chosen as explained below:

- Model “ Λ CDM-P” refers to a cosmological constant scenario with Ω_m and h fixed to Planck cosmology [36].
- Model “ $SEoS$ -P” refers to the best fit values for the parameters in equation (2) as obtained in [32] while maintaining Ω_m and h to a Planck cosmology [36].
- Model “ CPL -P” refers to the scenario where we adopt the CPL limit of the above solution, meaning we keep $\{w_0, w_i\} = \{-0.92, -0.99\}$, as obtained in [32] and $\{\Omega_m, h\}$ fixed to a Planck cosmology [36], but we make $z_T = q = 1$.
- Finally, Model “ $SEoS$ -bf” refers to the best fit values for the parameters in equation (2) (i.e. $\{w_0, w_i, q, z_T\} = \{-0.92, -0.99, 9.97, 0.28\}$) with Ω_m and h also fixed to the best fit values obtained in [32].

The corresponding expansion histories for those models are shown in figure 2, where we plot $H(a)/H_0$ and the relative ratio from models $SEoS$ -P, CPL -P and $SEoS$ -bf to Λ CMD-P in the bottom panel: $\Delta H/H_\Lambda \equiv (H - H_\Lambda)/H_\Lambda$.

A. Growth function

In the case where $\delta_{DE} = 0$, equation 6 reduces to:

$$a^2 \frac{d^2 \delta_m(a)}{da^2} + a \left(3 + \frac{\dot{H}}{H^2} \right) \frac{d\delta_m(a)}{da} - \frac{3}{2} \Omega_m \delta_m(a) = 0. \quad (7)$$

This can be solved by setting initial conditions in the matter dominated era, $a_{ini} = 10^{-3}$, since we know that during this epoch, the solution for the growth function is $\delta_m(a) = a$, we have $\delta_m(a_{ini}) = a_{ini} = 10^{-3}$ and $\delta'_m(a_{ini}) = 1$.

A solution for equation (7) can be given up to a normalization. We choose to normalize it such that $D_m^{(+)}(a) = 1$ at $a = a_{ini}$, so we enhance the differences arising at present time. This is shown in Figure 3a for the models under consideration. Once we have the solution to equation (7), we can also find the logarithmic growth function, $f(a) \equiv \frac{d \log \delta_m(a)}{d \log a}$ (see fig. 3b).

To get a better idea of the effect of different dark energy models in the growth functions $D^{(+)}(a) \equiv$

$\frac{\delta_m(a)}{\delta_m(a_{ini})}$, $f(a)$, we take the relative difference to a Λ CDM - P scenario: $\Delta \mathcal{F}/\mathcal{F}_\Lambda \equiv \frac{\mathcal{F} - \mathcal{F}_\Lambda}{\mathcal{F}_\Lambda}$ with $\mathcal{F} = \{D_m^{(+)}, f(a)\}$ and \mathcal{F}_Λ the solution assuming Λ CDM-P as background model. This is show, for instance, in the bottom panel of plots 3a and 3b, respectively.

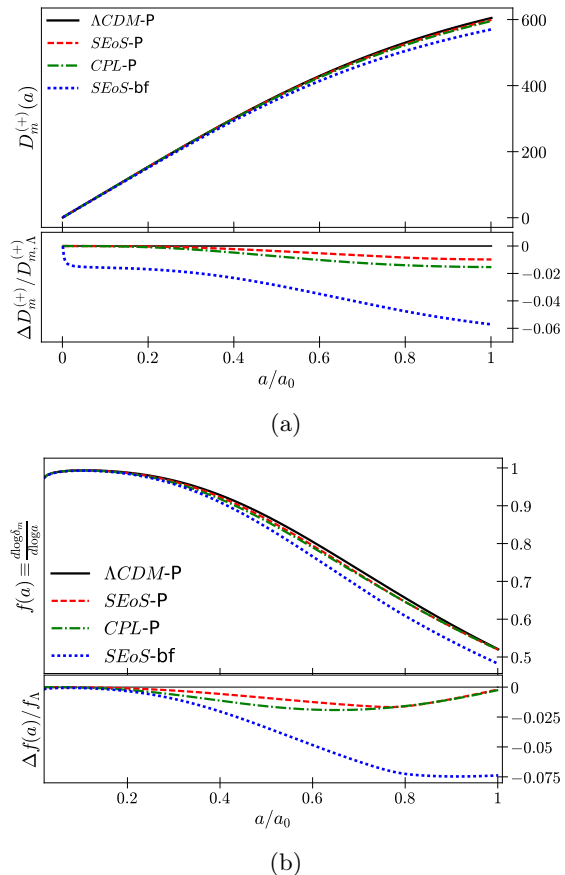


FIG. 3: [Color online] (a) Evolution of matter overdensities normalized to the initial time, $D_m^{(+)}(a)$, and (b) logarithmic growth function, $f(a)$ for the models in table I. The bottom panel displays the relative difference to Λ CDM-P solution: $\Delta \mathcal{F}/\mathcal{F}_\Lambda \equiv \frac{\mathcal{F} - \mathcal{F}_\Lambda}{\mathcal{F}_\Lambda}$ with \mathcal{F} representing $D_m^{(+)}(a)$ or $f(a)$, respectively.

Regarding the results for $D_m^{(+)}$ we find deviations from Λ CDM that are of order:

- of 1% at $z = 0$ if we assume model $SEoS$ -P as our DE component,
- of order 1.5%, for CPL -P,
- and of order of 6% at $z = 0$ taking $SEoS$ -bf.

The differences in $\Delta f(a)/f_\Lambda$ are consistent, showing deviations at percent level: the fastest expan-

sion rate corresponds to *SEoS*-bf model (as indicated in figure 2), followed by *CPL*-P and *SEoS*-P. Hence, we obtained a slower growth of structure and a slower logarithmic growth rate in *SEoS*-bf model (followed by *CPL*-P and *SEoS*-P).

It is important to note that the discrepancy between Λ CDM and a dynamic form of dark energy is bigger for the CPL scenario than the case $\{w_0, w_i, q, z_T\} = \{-0.92, -0.99, 9.97, 0.28\}$ (Model *CPL*-P versus Model *SEoS*-P in figure 3). This is due to the fact that the CPL limit has $z_T = 1$, which implies that for this case $w(z) \rightarrow -0.92$ for $z \leq 1$, whereas Model *SEoS*-P has a later transition redshift, implying that $w(z) \rightarrow -0.92$ for $z \leq 0.28$.

B. Linear matter power spectrum

By means of a modified version of CAMB [37] in which we incorporated “SEoS” as expansion model and considered negligible DE perturbations, we computed the linear matter power spectrum, $P(k)$, which is calculated in the synchronous gauge, used internally by the code.

1. *SEoS*: DE dynamics only

Our results are shown in Figure 4. In this we show the linear matter spectrum for Λ CDM and *SEoS*-P (figure 4a) and their ratio $\Delta P(k)/P_\Lambda \equiv (P(k) - P_{\Lambda\text{CDM}}(k))/P_{\Lambda\text{CDM}}(k)$ for different redshift values ($z = 0$, $z = z_T = 0.28$, $z = 2z_T = 0.56$, and $z = 1$).

We notice a decrease in amplitude for all Fourier modes, of order 0.5% (1.7%) for redshift values $z = 1$ ($z = 0$), respectively (see figure 4a). This is to be expected since we have seen that a consequence of the dynamics of *SEoS*-P is an Universe that expands more rapidly as compared to one dominated by a cosmological constant. The effect appears after the transition has occurred, since for $z > z_T$, our EoS behaves as a cosmological constant term ($w_i \approx -1$). In addition to this decrease, we notice a bump in $k \approx 6 \times 10^{-4} h^{-1}/\text{Mpc}$ for $\Delta P(k)/P_\Lambda|_{z=0}$. This is better depicted in figure 4b, where we show the ratio between *SEoS*-P and Λ CDM-P for power spectra after the transition has occurred ($z < z_T$). From the bottom panel of figure 4a we notice the bump appears only after the transition has occurred, and in figure 4b we see it increases as $z \rightarrow 0$. We can know which modes are entering to the horizon during and after the transition epoch of $z_T = 0.28$.

Using $h = 0.6774$ we have $k_T \equiv a_T H(a_T) = 1.403 \times 10^{-4} h^{-1}/\text{Mpc}$ (shown as a red dotted vertical line in figure 4b) with $a_T = 1/(1 + z_T)$. Which means

that modes $k < k_T$ enter into the horizon after the abrupt transition took place.

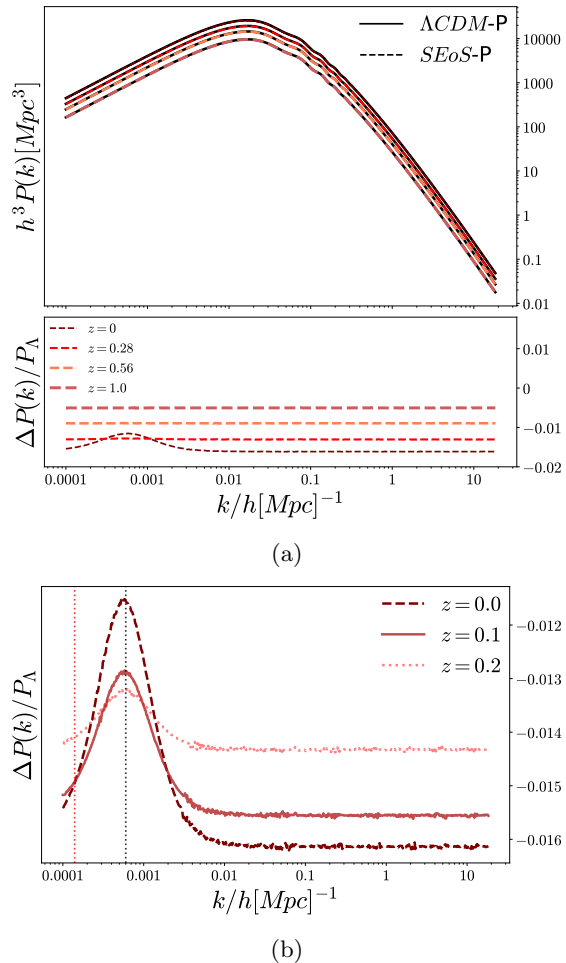


FIG. 4: [Color online] (a) Linear matter power spectra for Models I and II (Table I) at different redshift values ($z = 0$, $z = z_T = 0.28$, $z = 2z_T = 0.56$, and $z = 1$) and the ratio from “*SEoS*-P” to Λ CDM. (b) Zoom-in of the previous plot showing $\Delta P(k)/P_\Lambda(k)$ for $z < z_T$: $z = 0, 0.1, 0.2$. The (red) vertical line at $k = 1.403 \times 10^{-4} h^{-1}/\text{Mpc}$ indicates the mode associated to the transition redshift ($z_T = 0.28$), $k_T = a_T H(a_T)$, whereas the (black) vertical line in $k \approx 6 \times 10^{-4} h^{-1}/\text{Mpc}$, indicates the maximum of the bump in $\Delta P(k)/P_\Lambda(k)$.

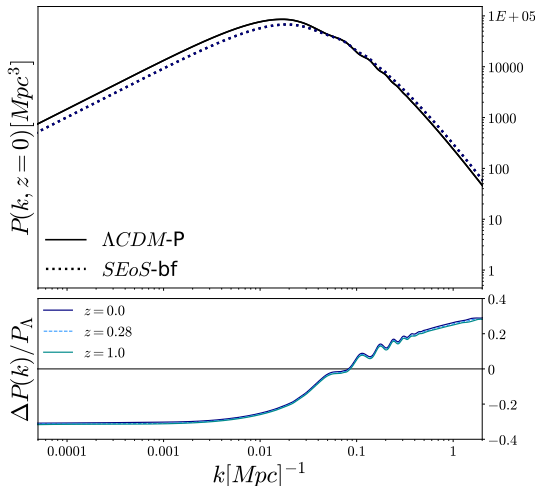


FIG. 5: [Color online] (Upper panel) Linear matter power spectra at present time for *SEoS*-bf and Λ CDM-P from Table I. (Bottom panel) Ratio between *SEoS*-bf to Λ CDM-P at different redshift values ($z = 0$, $z = z_T = 0.28$, $z = 2z_T = 0.56$, $z = 1$).

2. *SEoS*: best fit value

Now, in figure 5 we show the difference in power spectrum between Λ CDM and the model *SEoS*-bf, in which not only the dynamics of DE is different but also the amount of matter, $\Omega_m^{(0)}$ and Hubble factor H_0 . Notice that in this case we report $P(k)[\text{Mpc}^3]$ and $k[\text{Mpc}^{-1}]$ to take into account the fact that each model has its corresponding h value. It is important to recall that we have set the same initial power spectra for all our models, even in the *SEoS*-bf case.

The bottom panel of figure 5 shows a decrease in power spectrum for small modes ($k \leq 0.01/\text{Mpc}$), and a similar increase in amplitude for the biggest modes ($k \geq 1/\text{Mpc}$). Those modes ($k \geq 1/\text{Mpc}$) entered first into the horizon and given that the Universe in *SEoS*-bf model expands more rapidly than in Λ CDM-P (see figure 2), they have had more time to evolve and accrete mass, hence, generating more power in the *SEoS*-bf power spectrum.

It is customary to express the matter power spectrum at late times in terms of the initial power spectrum, the matter transfer function and the growth function [38]:

$$P(k, a) = 2\pi^2 \delta_H^2 \frac{k^n}{H_0^{n+3}} T^2(k) \left[\frac{D_1(a)}{D_1(a=1)} \right]^2, \quad (8)$$

and since we know that the primordial power spectrum has been kept the same in all models tested,

and the transfer function is roughly the same ($\approx 9/10$) for small modes, we can estimate the amount of deviation for small modes from $P_{SEoS}(k)/P_\Lambda$ to be of the order $\frac{(D_{1,seos}/D_{1,\Lambda})^2}{(H_{0,seos}/H_{0,\Lambda})^4}$. From results in figures 2 and 3a we get $\frac{(D_{1,seos}/D_{1,\Lambda})^2}{(H_{0,seos}/H_{0,\Lambda})^4} = \frac{(0.95)^2}{(1.08)^4} \approx 0.66$ which in turns means $\Delta P(k) \approx -33\%$, in agreement with figure 5.

C. Large scale structure

Galaxy redshift maps constrain the combination $f\sigma_8(z)$ using measurements of the redshift space distortions (RSD). So, in order to have an insight on the possible implications of the model into the growth of structure at large scales, we consider the $f\sigma_8(z)$ function and compare with some of the current observational constraints reported in the literature and listed below. This is shown in figure 6. We added the observational points reported by the following surveys: 6dFG [39], SDSS MGS [40], SDSS-LRG [41], BOSS-LOWZ and BOSS-CMASS [42], WIGGLE-z [43] and the VIPERS [44]. As previously mentioned, we show the relative difference $\Delta\mathcal{F}/\mathcal{F}_\Lambda \equiv \frac{\mathcal{F}-\mathcal{F}_\Lambda}{\mathcal{F}_\Lambda}$ with $\mathcal{F} = \{f\sigma_8(z), dn/d\log M(z=0)\}$ and \mathcal{F}_Λ the solution assuming Λ CDM-P as background model.

From this result we see that model *SEoS*-bf predicts a larger value for $f\sigma_8(z)$ at all redshift values $z \in [0, 1.5]$. This increase (of order $\Delta f\sigma_8 \sim 20\%$) makes model *SEoS*-bf in discordance with the current observations of $f\sigma_8(z)$, whereas *SEoS*-P and its *CPL* limit are within observational error bars and deviate from Λ CDM-P by less of 3%, in conformity with our previous results, in particular, we see that the difference in $\Delta f\sigma_8(z)$ is in agreement with the result shown in figure 3b.

Additionally we consider the fractional number of collapsed structures by means of the Press-Schechter formalism, which describes the matter over-density field in real space by a smooth gaussian field whose variance on a sphere of radius R is σ_R^2 [45]. In this formalism, the number of collapsed objects per unit volume with mass between M and $M + dM$ is given by:

$$dn = -\sqrt{\frac{2}{\pi}} \frac{d\sigma_R}{dM} \left(\frac{\bar{\rho}_m \delta_c}{M \sigma_R^2} \right) \exp\left(-\frac{\delta_c^2}{2\sigma_R^2}\right) dM \quad (9)$$

where $\delta_c = 1.686$, the linear over-density at collapse is set to the value for Λ CDM since the dependence on cosmology is not strong [46]. In figure 7 we show the differential mass function for the models considered and their relative ratio to Λ CDM-P model.

In this case we notice that *SEoS*-bf model predicts a decrease in the number of smalls structures

(masses $M \sim \mathcal{O}(10^{10} M_\odot)$) by 10% compared to Λ CDM scenario, and an increase of 30% ($M \sim \mathcal{O}(10^{14} M_\odot)$) and as big as 50% for the biggest collapsed structures ($M \geq 4 \times 10^{14} M_\odot$).

For *SEoS-P* and *CPL-P* models, the behavior is the opposite: we find an increase in the number of small objects (masses $M \leq 6 \times 10^{12} M_\odot$) of order 1–2% and a decrease in the number of big structures ($M \geq 5 \times 10^{14} M_\odot$) of $\sim 3\%$ for *SEoS-P* and 6% for its *CPL* limit.

We recall that the mass M is inversely proportional to the wave-number since $M \propto R^3$ and $R = \pi/k$, indicating that large masses correspond to small modes (large scales) and vice versa. In *SEoS-bf* model, additionally to the DE dynamics we have a different value for $\bar{\rho}_m$ than in Λ CDM (see equation(9)), which impacts importantly the mass function, as we have just discussed. For models *SEoS-P* and *CPL-P*, however, the matter content is the same and hence when we compare the differential mass function at a particular mass scale we are also comparing that function at the same mode. Moreover, since the age of the Universe is practically the same in models I-III (table I), the resulting discrepancies previously discussed mean that large structures take more time to form in a *SEoS* model, while small objects form more quickly.

As a consequence we can say that we would expect to observe less massive galaxy clusters and more light structures (isolated galaxies and poorly populated clusters) in *SEoS-P* or *CPL-P* universe.

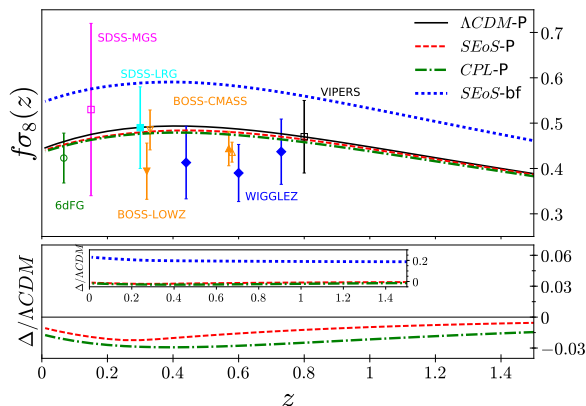


FIG. 6: [Color online] Predictions on $f\sigma_8(z)$ for model of table I. On top, we added the observational points reported by several surveys [39–44]. The bottom panel shows the relative difference with respect to Λ CDM-P.

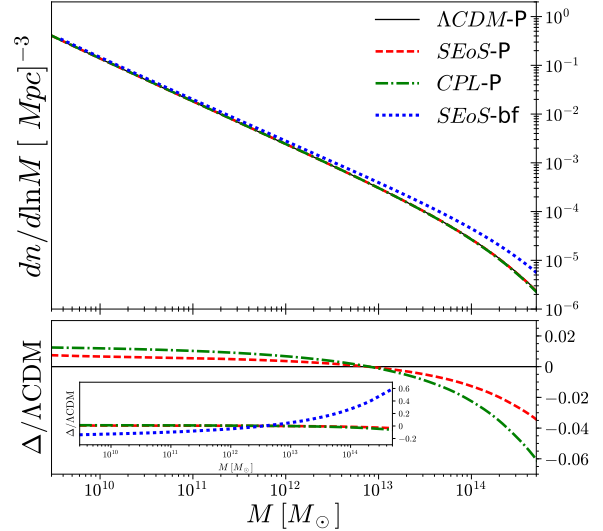


FIG. 7: [Color online] Differential mass function $dn/d \ln M$ for models of table I at $z = 0$. The bottom panel shows the relative difference to Λ CDM-P.

IV. CONCLUSIONS

We studied a DE model with the characteristic of a step transition between two pivotal values. This model was previously analyzed at background level and its free parameters were tested against observations such as the latest local determination of H_0 , the BAO peak and the angular distance to the CMB [32], and constrained its free parameters to: ($w_0 = -0.92$, $w_i = -0.99$, $q = 9.97$, $z_T = 0.28$). This work investigates how a steep transition in the DE EoS can affect the growth of structure, and we restricted ourselves to the case of a smooth DE component.

We find that the effect of a SEoS for DE in structure formation can basically be separated into two phenomena: **1)** On one hand the presence of a dynamical dark energy changes the expansion of the background, leading to different growth rates and affecting the matter fluctuations **2)** While on the other hand, the change in Ω_m as well the Hubble rate (according to the BFV obtained previously) has a bigger impact than just the DE dynamics, modifying the observable quantities such as $P(k)$, $f\sigma_8(z)$, and $dn/d \log M$ beyond the current observational constraints.

In the first case we find that the change in the Hubble expansion of 1.5% percent at the transition epoch ($z_T = 0.28$ or $z_T = 1$ in “*SEoS-P*” or “*CPL-P*”, respectively), impacts the growth functions in an equivalent amount, diminishing the growth of struc-

ture at linear order by 1.5% – 2% (figure 3). This consequently imprints into $f\sigma_8(z)$ as a decrease of $\sim 2 - 3\%$ and lies in agreement with RSD observational measurements from surveys [39–44]. As for the differential mass function, $dn/d\log M(z=0)$, we find as a prediction, a slight increment in the number of small collapsed objects of order 1% (2%) and a decrement in the number of large structures or order 3% (6%) for *SEoS-P (CPL-P)* model.

The *CPL* limit of *SEoS-P* model (which means taking $z_T = q = 1$ in equation (2)), consistently shows bigger differences from Λ CDM model than *SEoS-P*, as a result of an earlier (yet smooth) transition from $w_i \approx -1$ to a bigger value $w_0 = -0.92$, which implies the DE dilutes first in *CPL-P* model. As for the matter power spectrum, we see that the change in expansion rate affects all Fourier modes equally, decreasing the amplitude of power spectrum by $\sim 1.6\%$ at $z=0$. Additionally to this effect, we notice the appearance of a bump in the modes close to those entering near the steep transition, in the linear regime ($k \sim 10^{-4}h^{-1}/Mpc$), which appears only after the transition took place ($z < z_T$) and increases amplitude as $z \rightarrow 0$.

In the second case, this is, for *SEoS-P* model, we find an interplay between having an Universe with $\Delta\omega_c = 0.1568/0.1198 \sim 30\%$ bigger than in a Λ CDM scenario, with the change in the expansion rate, such that the clustering is prevented at large scales (small Fourier modes or large masses) and enhanced at enhanced at small scales (large Fourier modes or small masses). See for instance figures 5

and 7. From the differential mass function, for instance, the prediction is that the number of collapsed objects decreases (increases) by approximately 10% (50 – 60%) for light (the largest) structures. Lastly, the effect on $f\sigma_8(z)$, however implies that model *SEoS-bf* is not in agreement with RSD observational constraints.

To summarize, the study of dynamics of Dark Energy is a matter of profound implications for our understanding of the Universe and its physical laws. Studying the behavior of a model beyond background level is nowadays required given the important amount of data coming from redshift galaxy surveys and its potential to test discrepancies among a cosmological constant, fluids with negative pressure or modifications to the gravity sector. In this paper we have contributed towards that direction showing that the evolution of matter over-densities is sensitive to the parameters in equation (2), and a model with a steep transition such as the one explored in this paper can lead to interesting features in the growth of structure.

ACKNOWLEDGEMENTS

This project was done with funding from the CONACYT grant Fronteras de la Ciencia 000281 and PASPA-DGAPA UNAM. M.J. thanks Omar A. Rodríguez L. for computational help and the group of Extragalactic Astronomy and Cosmology of Institute of Astronomy UNAM for fruitful discussions.

-
- [1] Steven Weinberg. The cosmological constant problem. *Rev. Mod. Phys.*, 61:1–23, Jan 1989. doi:10.1103/RevModPhys.61.1.
 - [2] N. Aghanim et al. Planck 2018 results. VI. Cosmological parameters. 2018.
 - [3] D. M. Scolnic et al. The Complete Light-curve Sample of Spectroscopically Confirmed SNe Ia from Pan-STARRS1 and Cosmological Constraints from the Combined Pantheon Sample. *Astrophys. J.*, 859(2):101, 2018. doi:10.3847/1538-4357/aab9bb.
 - [4] F. Beutler, C. Blake, M. Colless, D. H. Jones, L. Staveley-Smith, L. Campbell, Q. Parker, W. Saunders, and F. Watson. The 6dF Galaxy Survey: baryon acoustic oscillations and the local Hubble constant. *MNRAS*, 416:3017–3032, October 2011. doi:10.1111/j.1365-2966.2011.19250.x.
 - [5] Ashley J. Ross, Lado Samushia, Cullan Howlett, Will J. Percival, Angela Burden, and Marc Manera. The clustering of the SDSS DR7 main Galaxy sample I. A 4 per cent distance measure at $z = 0.15$. *Mon. Not. Roy. Astron. Soc.*, 449(1):835–847, 2015. doi:10.1093/mnras/stv154.
 - [6] Nikhil Padmanabhan, Xiaoying Xu, Daniel J. Eisenstein, Richard Scalzo, Antonio J. Cuesta, Kushal T. Mehta, and Eyal Kazin. A 2 per cent distance to $z = 0.35$ by reconstructing baryon acoustic oscillations i. methods and application to the sloan digital sky survey. *Monthly Notices of the Royal Astronomical Society*, 427(3):2132–2145, 2012. ISSN 1365-2966. doi:10.1111/j.1365-2966.2012.21888.x.
 - [7] Shadab Alam et al. The clustering of galaxies in the completed SDSS-III Baryon Oscillation Spectroscopic Survey: cosmological analysis of the DR12 galaxy sample. *Submitted to: Mon. Not. Roy. Astron. Soc.*, 2016.
 - [8] Eyal A. Kazin et al. The WiggleZ Dark Energy Survey: improved distance measurements to $z = 1$ with reconstruction of the baryonic acoustic feature. *Mon. Not. Roy. Astron. Soc.*, 441(4):3524–3542, 2014. doi:10.1093/mnras/stu778.
 - [9] Andreu Font-Ribera et al. Quasar-Lyman α Forest Cross-Correlation from BOSS DR11 : Baryon Acoustic Oscillations. *JCAP*, 1405:027, 2014. doi:10.1088/1475-7516/2014/05/027.

- [10] Timothe Delubac et al. Baryon acoustic oscillations in the Lyman α Forest of BOSS DR11 quasars. *Astron. Astrophys.*, 574:A59, 2015. doi:10.1051/0004-6361/201423969.
- [11] Yu Liang, Cheng Zhao, Chia-Hsun Chuang, Francisco-Shu Kitaura, and Charling Tao. Measuring Baryon Acoustic Oscillations from the clustering of voids. *Mon. Not. Roy. Astron. Soc.*, 459(4):4020–4028, 2016. doi:10.1093/mnras/stw884.
- [12] Michel Chevallier and David Polarski. Accelerating universes with scaling dark matter. *Int. J. Mod. Phys.*, D10:213–224, 2001. doi:10.1142/S0218271801000822.
- [13] Eric V. Linder. Exploring the expansion history of the universe. *Phys. Rev. Lett.*, 90:091301, 2003. doi:10.1103/PhysRevLett.90.091301.
- [14] Michael Doran and Georg Robbers. Early dark energy cosmologies. *JCAP*, 0606:026, 2006. doi:10.1088/1475-7516/2006/06/026.
- [15] Lawrence M Krauss, Katherine Jones-Smith, and Dragan Huterer. Dark energy, a cosmological constant, and type ia supernovae. *New Journal of Physics*, 9(5):141, 2007.
- [16] Eric V. Linder. Dark Energy in the Dark Ages. *Astropart. Phys.*, 26:16–21, 2006. doi:10.1016/j.astropartphys.2006.04.004.
- [17] D. Rubin et al. Looking Beyond Lambda with the Union Supernova Compilation. *Astrophys. J.*, 695:391–403, 2009. doi:10.1088/0004-637X/695/1/391.
- [18] J. Sollerman, E. Mörtzell, T. M. Davis, M. Blomqvist, B. Bassett, A. C. Becker, D. Cinabro, A. V. Filippenko, R. J. Foley, J. Frieman, P. Garnavich, H. Lampeitl, J. Marriner, R. Miquel, R. C. Nichol, M. W. Richmond, M. Sako, D. P. Schneider, M. Smith, J. T. Vanderplas, and J. C. Wheeler. First-Year Sloan Digital Sky Survey-II (SDSS-II) Supernova Results: Constraints on Nonstandard Cosmological Models. *Astrophys. J.*, 703:1374–1385, October 2009. doi:10.1088/0004-637X/703/2/1374.
- [19] M. J. Mortonson, W. Hu, and D. Huterer. Testable dark energy predictions from current data. *Phys. Rev. D*, 81(6):063007, March 2010. doi:10.1103/PhysRevD.81.063007.
- [20] Steen Hannestad and Edvard Mortsell. Cosmological constraints on the dark energy equation of state and its evolution. *JCAP*, 0409:001, 2004. doi:10.1088/1475-7516/2004/09/001.
- [21] H. K. Jassal, J. S. Bagla, and T. Padmanabhan. WMAP constraints on low redshift evolution of dark energy. *Mon. Not. Roy. Astron. Soc.*, 356:L11–L16, 2005.
- [22] Jing-Zhe Ma and Xin Zhang. Probing the dynamics of dark energy with novel parametrizations. *Phys. Lett.*, B699:233–238, 2011. doi:10.1016/j.physletb.2011.04.013.
- [23] Dragan Huterer and Michael S. Turner. Probing the dark energy: Methods and strategies. *Phys. Rev.*, D64:123527, 2001. doi:10.1103/PhysRevD.64.123527.
- [24] Jochen Weller and Andreas Albrecht. Future supernovae observations as a probe of dark energy. *Phys. Rev.*, D65:103512, 2002. doi:10.1103/PhysRevD.65.103512.
- [25] Zhiqi Huang, J. Richard Bond, and Lev Kofman. Parameterizing and Measuring Dark Energy Trajectories from Late-Inflatons. *Astrophys. J.*, 726:64, 2011. doi:10.1088/0004-637X/726/2/64.
- [26] E. M. Barboza, Jr. and J. S. Alcaniz. A parametric model for dark energy. *Phys. Lett.*, B666:415–419, 2008. doi:10.1016/j.physletb.2008.08.012.
- [27] Luisa G. Jaime, Mariana Jaber, and Celia Escamilla-Rivera. New parametrized equation of state for dark energy surveys. *Phys. Rev.*, D98(8):083530, 2018. doi:10.1103/PhysRevD.98.083530.
- [28] Michael R. Blanton et al. Sloan digital sky survey iv: Mapping the milky way, nearby galaxies, and the distant universe. *The Astronomical Journal*, 154(1):28, 2017.
- [29] DESI collaboration. Desi final design report part i: Science, targeting, and survey design, 2016. [Online; accessed 30-September-2018].
- [30] LSST Science Collaboration, P. A. Abell, J. Allison, S. F. Anderson, J. R. Andrew, J. R. P. Angel, L. Armus, D. Arnett, S. J. Asztalos, T. S. Axelrod, and et al. LSST Science Book, Version 2.0. *ArXiv e-prints*, arXiv:0912.0201, December 2009.
- [31] R. Laureijs, J. Amiaux, S. Arduini, J. . Auguères, J. Brinchmann, R. Cole, M. Cropper, C. Dabin, L. Duvet, A. Ealet, and et al. Euclid Definition Study Report. *ArXiv e-prints*, arXiv:1110.3193, October 2011.
- [32] Mariana Jaber and Axel de la Macorra. Probing a Steep EoS for Dark Energy with latest observations. *Astropart. Phys.*, 97:130–135, 2018. doi:10.1016/j.astropartphys.2017.11.007.
- [33] Pia Mukherjee, Martin Kunz, David Parkinson, and Yun Wang. Planck priors for dark energy surveys. *Phys. Rev. D*, 78:083529, Oct 2008. doi:10.1103/PhysRevD.78.083529.
- [34] P. A. R. Ade et al. Planck 2015 results. XIV. Dark energy and modified gravity. *Astron. Astrophys.*, 594:A14, 2016. doi:10.1051/0004-6361/201525814.
- [35] Adam G. Riess et al. A 2.4% Determination of the Local Value of the Hubble Constant. *Astrophys. J.*, 826(1):56, 2016. doi:10.3847/0004-637X/826/1/56.
- [36] P. A. R. Ade et al. Planck 2015 results. XIII. Cosmological parameters. *Astron. Astrophys.*, 594:A13, 2016. doi:10.1051/0004-6361/201525830.
- [37] Antony Lewis, Anthony Challinor, and Anthony Lasenby. Efficient computation of CMB anisotropies in closed FRW models. *Astrophys. J.*, 538:473–476, 2000. doi:10.1086/309179.
- [38] Scott Dodelson. *Modern cosmology*. Academic Press, San Diego, CA, 2003.
- [39] Florian Beutler, Chris Blake, Matthew Colless, D. Heath Jones, Lister Staveley-Smith, Gregory B. Poole, Lachlan Campbell, Quentin Parker, Will Saunders, and Fred Watson. The 6dF Galaxy Survey: $z \approx 0$ measurements of the growth rate and σ_8 . *MNRAS*, 423(4):3430–3444, Jul 2012. doi:10.1111/j.1365-2966.2012.21136.x.

- [40] Cullan Howlett, Ashley J. Ross, Lado Samushia, Will J. Percival, and Marc Manera. The clustering of the sdss main galaxy sample ii: mock galaxy catalogues and a measurement of the growth of structure from redshift space distortions at $z=0.15$. *MNRAS*, 449(1):848–866, 5 2015. ISSN 0035-8711. doi: 10.1093/mnras/stu2693.
- [41] Akira Oka, Shun Saito, Takahiro Nishimichi, Atsushi Taruya, and Kazuhiro Yamamoto. Simultaneous constraints on the growth of structure and cosmic expansion from the multipole power spectra of the SDSS DR7 LRG sample. *Mon. Not. Roy. Astron. Soc.*, 439:2515–2530, 2014. doi: 10.1093/mnras/stu111.
- [42] Hector Gil-Marn et al. The clustering of galaxies in the SDSS-III Baryon Oscillation Spectroscopic Survey: RSD measurement from the LOS-dependent power spectrum of DR12 BOSS galaxies. *Mon. Not. Roy. Astron. Soc.*, 460(4):4188–4209, 2016. doi: 10.1093/mnras/stw1096.
- [43] Chris Blake, Sarah Brough, Matthew Colless, Warwick Couch, Scott Croom, Tamara Davis, Michael J. Drinkwater, Karl Forster, Karl Glazebrook, and Ben Jelliffe. The WiggleZ Dark Energy Survey: the selection function and $z = 0.6$ galaxy power spectrum. *MNRAS*, 406(2):803–821, Aug 2010. doi: 10.1111/j.1365-2966.2010.16747.x.
- [44] S. de la Torre et al. The VIMOS Public Extragalactic Redshift Survey (VIPERS). Galaxy clustering and redshift-space distortions at $z=0.8$ in the first data release. *Astron. Astrophys.*, 557:A54, 2013. doi: 10.1051/0004-6361/201321463.
- [45] W. H. Press and P. Schechter. Formation of Galaxies and Clusters of Galaxies by Self-Similar Gravitational Condensation. *Astrophys. J.*, 187:425–438, February 1974. doi:10.1086/152650.
- [46] F. Pace, J.-C. Waizmann, and M. Bartelmann. Spherical collapse model in dark-energy cosmologies. *Monthly Notices of the Royal Astronomical Society*, 406(3):1865–1874, 08 2010. ISSN 0035-8711. doi:10.1111/j.1365-2966.2010.16841.x.